33rd Annual International Conference of the IEEE EMBS
Boston, Massachusetts USA, August 30 - September 3, 2011

Kalman filter-based time-varying cortical connectivity analysis of newborn EEG

A.H. Omidvarnia[1], M. Mesbah[1], M. S. Khlif[1], J.M. O'Toole[2], P.B. Colditz[1], B. Boashash[1,3]

Abstract— **Multivariate Granger causality in the time-frequency domain as a representation of time-varying cortical connectivity in the brain has been investigated for the adult case. This is, however, not the case in newborns as the nature of the transient changes in the newborn EEG is different from that of adults. This paper aims to evaluate the performance of the time-varying versions of the two popular Granger causality measures, namely Partial Directed Coherence (PDC) and direct Directed Transfer Function (dDTF). The parameters of the time-varying AR, that models the inter-channel interactions, are estimated using Dual Extended Kalman Filter (DEKF) as it accounts for both non-stationarity and non-linearity behaviors of the EEG. Using simulated data, we show that fast changing cortical connectivity between channels can be measured more accurately using the time-varying PDC. The performance of the time-varying PDC is also tested on a neonatal EEG exhibiting seizure.**

I. PREVIOUS WORK

Studies on the dynamical interrelations between different brain structures may potentially identify neural mechanisms of pathophysiological diseases and, therefore, improve clinical interventions [1]. Due to its non-invasive nature, high temporal resolution and low cost, scalp EEG remains the preferred neural activity monitoring tool for investigating temporo-spatial connectivity of the different cortical areas.

In essence, the nature of the transient changes in the newborn EEG is different from that of adults. Many of the neonatal EEG patterns have completely different medical implications than when observed in later ages [1]. Moreover, rapid maturational changes are observed in the newborn brain until early infancy [2]. This imposes high inter- and intra-individual differences in the EEG transients during the neonatal period [3]. In fact, some EEG features that are normal at a certain stage of development become abnormal in a later stage [1]. As a consequence, interactions between the brain regions in neonates differ from those of the mature brain [2].

[1] Manuscript received April 15, 2011.
A.H. Omidvarnia (corresponding author, a.omidvarnia@uq.edu.au), M. Mesbah (m.mesbah@uq.edu.au), M.S. Khlif (m.khlif@uq.edu.au), P.B. Colditz (p.colditz@uq.edu.au) and B. Boashash (b.boashash@uq.edu.au) are with the Clinical Research Centre, The University of Queensland, Brisbane, Australia.
[2] J.M. O' Toole (j.otoole@ieee.org) is with DeustoTech, University of Deusto, Bilbao, Spain.
[3] B. Boashash is also with Qatar University College of Engineering, Doha, Qatar.

Multivariate autoregressive (MVAR) process, as a linear representation of multichannel EEG data, is able to model interactions between EEG channels in the form of linear difference equations [4]. By using this EEG representation, not only can the direction of the information flow between channels be inferred, but also the direct or indirect influences detected. Directed Coherence [4], Partial Directed Coherence (PDC) [4], Directed Transfer Function (DTF) [5] and direct Directed Transfer Function (dDTF) [6] are MVAR-based measures which have been introduced to determine directional influence in multivariate systems.

The above measures assume that the underlying signals are stationary and that their interactions are constant over time. However, EEG signals are non-stationary [7, 8]. This implies that the mutual influence of brain cortical regions and, therefore, those of EEG channels do not necessarily show a stationary behavior. Therefore, time-varying forms of connectivity measures should be used.

In this paper, nonstationary PDC and dDTF measures are computed for the simulated data using Dual Extended Kalman Filter to estimate the coefficients of the MVAR model. Then, the PDC measure is extracted from the neonatal EEG signals and the results are discussed. Previous studies have shown that Dual Extended Kalman Filter (DEKF) [9] can accurately track fast changing parameters of MVAR models [10]. The aim of the study is to investigate appropriate time-frequency representations of cortical connectivity during neonatal EEG seizures.

The remainder of the paper is organized as follows. Section 2 describes the DEKF as well as the time-varying PDC and dDTF measures based on DEKF. In section 3, results from using simulated and EEG data are presented. Section 4 concludes the paper.

II. METHODS

A. The model

For a time series $\boldsymbol{y}(n) \in \mathbb{R}^N$, a time-varying MVAR model of order p is defined as:

$$\begin{bmatrix} y_1(n) \\ \vdots \\ y_N(n) \end{bmatrix} = \sum_{r=1}^{p} \boldsymbol{A}_r(n) \begin{bmatrix} y_1(n-r) \\ \vdots \\ y_N(n-r) \end{bmatrix} + \begin{bmatrix} w_1(n) \\ \vdots \\ w_N(n) \end{bmatrix} \quad (1)$$

where $\boldsymbol{w} = [w_1 \cdots w_N]^T$ is a white noise vector. The matrices $\mathbf{A}_r$ are given by:

$$\boldsymbol{A}_r(n) = \begin{bmatrix} a_{11}^r(n) & \cdots & a_{1N}^r(n) \\ \vdots & \ddots & \vdots \\ a_{N1}^r(n) & \cdots & a_{NN}^r(n) \end{bmatrix} \quad (2)$$

for r = 1, …, p. The parameter $a_{ij}^{r}(n)$ reflects the time-varying linear relationship between channel i and channel j at the delay r. In the stationary case, the optimum order p of MVAR models can be estimated using different methods such as Akaike Information Criterion (AIC) and Schwarz's Bayesian Criterion (SBC) [11]. The model order selection is not straightforward for time-varying MVAR models, as this order can vary over time. In this study, the optimal model order is estimated using the ARFIT module [11] which evaluates the SBC for a range of p values over the entire data and is kept constant during the process.

B. Parameter estimation using DEKF

The DEKF [9] adapts two interlaced Extended Kalman filters, one for state estimation and the other for parameter estimation. The equivalent state space can be presented as

$$\begin{cases} \boldsymbol{a}(n) = \boldsymbol{a}(n-1) + \boldsymbol{n}_a(n) \\ \boldsymbol{x}(n) = \boldsymbol{F}\big(\boldsymbol{a}(n-1), \boldsymbol{x}(n-1)\big) + \boldsymbol{n}_x(n) \\ \boldsymbol{y}(n) = \boldsymbol{C}\boldsymbol{x}(n) + \boldsymbol{n}_y(n) \end{cases} \tag{3}$$

where $\boldsymbol{n}_a$, $\boldsymbol{n}_x$ and $\boldsymbol{n}_y$ are zero-mean white Gaussian noises with covariance matrices $\boldsymbol{R}_a$, $\boldsymbol{R}_x$ and $\boldsymbol{R}_y$, respectively. The estimator generates approximate maximum-likelihood estimates of the states and model parameters of a noisy time series simultaneously. The state $\boldsymbol{x}$ and the output $\boldsymbol{y}$ are assumed to be generated by a nonlinear system of equations with additive state ($\boldsymbol{n}_x(n)$) and observation ($\boldsymbol{n}_y(n)$) noises, respectively. At the same time, a second state space formulation is introduced for the estimation of the time-varying parameter vector $\boldsymbol{a}$. For the case of an M-dimensional time-varying AR(p) model, the function $\boldsymbol{F}$ is linear and the state estimation part of the filter at time n can be formulated as follows [9]:

$$\begin{cases} \hat{\boldsymbol{x}}(n|n-1) = \hat{\boldsymbol{A}}(n-1)\hat{\boldsymbol{x}}(n-1) \\ \boldsymbol{P}_{\hat{x}}(n|n-1) = \hat{\boldsymbol{A}}(n-1)\boldsymbol{P}_{\hat{x}}(t-1)\hat{\boldsymbol{A}}^T(n-1) + \boldsymbol{R}_x \\ \boldsymbol{K}_x(n) = \boldsymbol{P}_{\hat{x}}(n|n-1)\boldsymbol{C}^T(\boldsymbol{C}\boldsymbol{P}_{\hat{x}}(n|n-1)\boldsymbol{C}^T + \boldsymbol{R}_y)^{-1} \\ \boldsymbol{P}_{\hat{x}}(n) = (\boldsymbol{I} - \boldsymbol{K}_x(n)\boldsymbol{C})\boldsymbol{P}_{\hat{x}}(n|n-1) \\ \hat{\boldsymbol{x}}(n) = \hat{\boldsymbol{x}}(n|n-1) + \boldsymbol{K}_x(n)(\boldsymbol{y}(n) - \hat{\boldsymbol{y}}(n)) \end{cases} \tag{4}$$

where $\boldsymbol{P}_{\hat{x}} \in \mathbb{R}^{Mp\times Mp}$ is the state estimation error covariance matrix, $\boldsymbol{K}_x \in \mathbb{R}^{Mp\times M}$ is the state's Kalman gain and $\boldsymbol{R}_x \in \mathbb{R}^{Mp\times Mp}$ and $\boldsymbol{R}_y \in \mathbb{R}^{M\times M}$ are state and output noise covariance matrices respectively. The vectors $\hat{\boldsymbol{y}} \in \mathbb{R}^{M\times 1}$ (estimated output) and $\hat{\boldsymbol{x}} \in \mathbb{R}^{Mp\times 1}$ (estimated state vector) and the matrices $\boldsymbol{A} \in \mathbb{R}^{Mp\times Mp}$ (MVAR parameters matrix) and $\boldsymbol{C} \in \mathbb{R}^{M\times Mp}$ (measurement matrix) are defined as:

$$\begin{gathered} \hat{\boldsymbol{y}}(n) = \boldsymbol{C}\hat{\boldsymbol{x}}(n|n-1) \\ \boldsymbol{x}^T(n) = [\boldsymbol{y}^T(n) \ \dots \ \boldsymbol{y}^T(n-p+1)] \\ \boldsymbol{A}(n) = \begin{bmatrix} \boldsymbol{A}_1(n) & \cdots & \cdots & \boldsymbol{A}_p(n) \\ \boldsymbol{I} & \boldsymbol{0} & \cdots & \boldsymbol{0} \\ \boldsymbol{0} & \boldsymbol{I} & \cdots & \boldsymbol{0} \\ \vdots & \ddots & \ddots & \vdots \\ \boldsymbol{0} & \cdots & \boldsymbol{I} & \boldsymbol{0} \end{bmatrix} \\ \boldsymbol{C} = [\boldsymbol{I}\ 0\ 0\ \dots\dots 0], \qquad \boldsymbol{I} = eye(M) \end{gathered} \tag{5}$$

The parameter estimation stage at time n is given by:

$$\begin{cases} \hat{\boldsymbol{a}}(n|n-1) = \hat{\boldsymbol{a}}(n-1) \\ \boldsymbol{P}_{\hat{a}}(n|n-1) = \lambda^{-1}\boldsymbol{P}_{\hat{a}}(n-1) \\ \boldsymbol{K}_a(n) = \boldsymbol{P}_{\hat{a}}(n|n-1)\boldsymbol{H}(n)^T(\boldsymbol{H}(n)\boldsymbol{P}_{\hat{a}}(n|n-1)\boldsymbol{H}(n)^T + \boldsymbol{R}_a)^{-1} \\ \boldsymbol{P}_{\hat{a}}(n) = (\boldsymbol{I} - \boldsymbol{K}_a(n)\boldsymbol{H}(n))\boldsymbol{P}_{\hat{a}}(n|n-1) \\ \hat{\boldsymbol{a}}(n) = \hat{\boldsymbol{a}}(n|n-1) + \boldsymbol{K}_a(n)\big(\boldsymbol{y}(n) - \hat{\boldsymbol{y}}(n)\big) \end{cases} \tag{6}$$

where $\boldsymbol{a} \in \mathbb{R}^{M^2p\times 1}$ is the vectorized $\boldsymbol{A}(n)$ containing all MVAR parameters, $\boldsymbol{P}_{\hat{a}} \in \mathbb{R}^{M^2p\times M^2p}$ is the parameter estimation error covariance matrix, $\boldsymbol{K}_a \in \mathbb{R}^{M^2p\times M}$ is the parameter's Kalman gain, $\boldsymbol{R}_a \in \mathbb{R}^{M\times M}$ is the parameter estimation error covariance matrix and $\boldsymbol{H} \in \mathbb{R}^{M\times M^2p}$ is defined as:

$$\boldsymbol{H}(n) = \boldsymbol{C}\frac{\partial(\hat{\boldsymbol{A}}\hat{\boldsymbol{x}})}{\partial\hat{\boldsymbol{A}}}|_{\hat{\boldsymbol{A}}(n-1)} \tag{7}$$

C. Time-varying PDC and dDTF measures

A number of time-varying connectivity measures can be defined based on the following transformation of the MVAR parameters ($\boldsymbol{A}_r(n)$) to the frequency domain:

$$\boldsymbol{A}(n,f) = I - \sum_{r=1}^{p} \boldsymbol{A}_r(n)z^{-r}|_{z=e^{i2\pi f}} \tag{8}$$

The time-varying version of the PDC [4] is defined as:

$$\pi_{ij}(n,f) \triangleq \frac{abs(\boldsymbol{A}_{ij}(n,f))}{\sqrt{\boldsymbol{a}_j^H(n,f)\boldsymbol{a}_j(n,f)}} \tag{9}$$

where $\boldsymbol{a}_j(n,f)$ is the j'th column and $\boldsymbol{A}_{ij}(n,f)$ is the ij'th element of the matrix $\boldsymbol{A}(n,f)$.

Also, the time-varying version of the dDTF [6] is obtained as the product of the time-varying full frequency DTF (ffDTF) [6]:

$$ffDTF_{ij}(n,f) = \frac{\boldsymbol{H}_{ij}(n,f)}{\sqrt{\sum_{f=1}^{F}\sum_{k=1}^{N}|\boldsymbol{H}_{ik}(n,f)|^2}} \tag{10}$$

and the time-varying partial coherence

$$pCOH_{ij}(n,f) = \frac{\boldsymbol{M}_{ij}^2(n,f)}{\boldsymbol{M}_{jj}(n,f)\boldsymbol{M}_{ii}(n,f)} \tag{11}$$

where $\boldsymbol{H}(n,f) = \boldsymbol{A}^{-1}(n,f)$ is the time-varying transfer function, F is the number of frequency points (depending on the sampling rate and the frequency range) and $M_{ij}(n,f)$ is the determinant of the minor matrix obtained by removing i'th row and j'th column of the cross power spectral density matrix $\boldsymbol{S}(n,f)$ defined as:

$$\boldsymbol{S}(n,f) = \boldsymbol{H}(n,f)\boldsymbol{\Sigma}(n)\boldsymbol{H}^*(n,f) \tag{12}$$

where $\boldsymbol{\Sigma}(n)$ denotes the time-varying estimation error covariance matrix. These two measures take values between 0 and 1 where high values in a certain frequency band reflect a directionally linear influence from channel j to channel i in that band ($\mathrm{CH_i} \leftarrow \mathrm{CH_j}$).

Time-varying PDC and dDTF can be computed based on the time-varying MVAR model fitted to the signal using Dual Extended Kalman Filtering. A surrogate data method with 50 realizations is then used to select the statistically significant values of the time-varying PDC and dDTF measures at 99% confidence level. All values below the confidence level are set to zero for illustration purposes. Surrogates are obtained by randomizing all samples of the signal to remove all causal relationships between them [12]. Because of the summation over frequencies in the denominator (Eq. 10), the dDTF function is usually much smaller than one. In this paper, dDTF values are focused in 0 to 0.005 for magnifying the result and obtaining a clear representation.

III. Results and Discussion

A. Data

1) Simulated data

The data is obtained from a 3-dimensional MVAR(2)-process, two damped stochastically driven oscillators (y_2 and y_3) and a stochastically driven relaxator y_1 (Eq. 13). This process has previously been used to evaluate time-varying directed interactions in multivariate neural data [10].

$$\begin{cases} y_1(n) = 0.59y_1(n-1) - 0.20y_1(n-2) + \\ \qquad b(n)y_2(n-1) + c(n)y_3(n-1) + w_1(n) \\ y_2(n) = 1.58y_2(n-1) - 0.96y_2(n-2) + w_2(n) \\ y_3(n) = 0.60y_3(n-1) - 0.91y_3(n-2) + w_3(n) \end{cases} \quad (13)$$

For a model of length L=5000 samples, parameters $b(n)$ and $c(n)$ are depicted in Fig. 1.

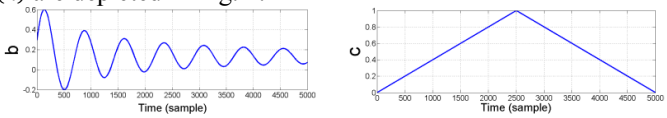

Fig. 1: Time course of the time-varying parameters in the model

2) Newborn EEG data

Seven monopolar channels (C_3, P_3, P_z, C_z, O_1, T_3, T_5) out of 14 channels recorded according to the 10-20 standard [13] were selected from a newborn EEG dataset. Beforehand, channel P_3 was identified by a matching pursuit-based algorithm [14] as the main location of seizure. Then, P_3 and its six peripheral electrodes were selected for further analysis. The results of the source localization will appear elsewhere. The data was recorded using a Medelec Profile system (Medelec, Oxford Instruments, Old Woking, UK) at 256 Hz sampling rate and marked by a pediatric neurologist from the Royal Children's Hospital, Brisbane, Australia. To decrease the computational load, the data was filtered using a 0.5-30 Hz band pass filter and down-sampled at the rate of 1/8.

B. Results

1) Simulated data

Figure 2 shows the most significant values of both time-varying PDC and dTDF measures at 99% level of significance after applying the surrogate data method. Both representations are able to reflect the time-varying partial connectivity from channel 2 to channel 1 and from channel 3 to channel 1. However, the dDTF plots represent two extra direct influences from channel 1 to channels 2 and 3, while corresponding PDC measures, namely, $\pi_{21}(n,f)$ and $\pi_{31}(n,f)$ reflect the immediate independence of $x_1(n)$ on $x_2(n)$ and $x_3(n)$. Also, the dDTF values are usually very small, as the summation over frequency in the denominator of the criterion makes all values much smaller than one. Moreover, multiplication of two smaller than 1 values makes the measure even smaller. In contrast, there is no problem with the time-varying PDC. For a better illustration of the dDTF measures, all significant values are zoomed in the interval of 0 to 0.005 in Fig. 2.

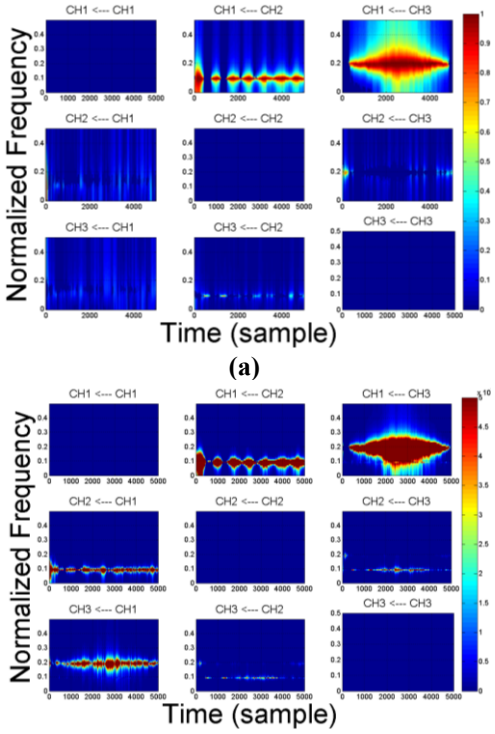

Fig. 2: PDC (panel **a**) and dDTF (panel **b**) of the model using the DEKF. The y-axis represents normalized frequency ([0 0.5] corresponding to [0 F_s/2]) and the x–axis represents time direction in terms of data samples.

2) Newborn EEG data

Due to the superiority of the time-varying PDC compared to the time-varying dDTF illustrated above, only the former measure was applied to the EEG data. Fig. 3 illustrates the time-varying PDC values extracted from a 10-sec ictal EEG epoch. The optimum AR model order was evaluated by Schwarz's Bayesian Criterion and fixed to 4 during the analysis. Based on visual inspection of the plots in Fig. 3 for all pairs of channels, a directed path graph can be suggested as the model of the seizure propagation within the seven utilized electrodes for this particular infant (Fig. 4). Note that the relationships within the graph are time-varying.

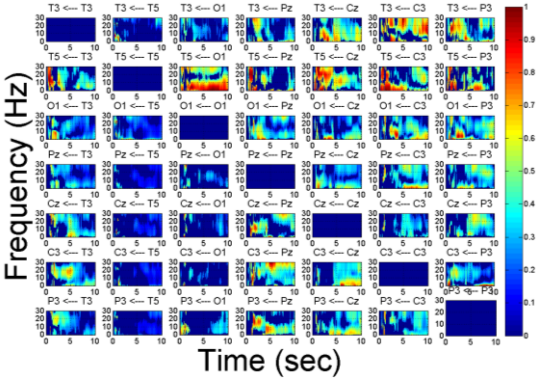

Fig. 3: PDC measure of the EEG data. The y-axis spans frequencies from zero to 30 Hz and the x–axis represents time direction.

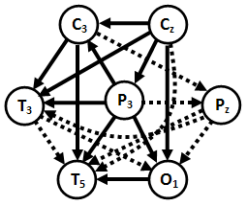

Fig. 4: Time-averaged static directed graph based on the time-varying PDC measure for the newborn ictal EEG data. Solid arrows show stronger relations, while dashed ones reflect weak interactions (i.e., sparse regions with medial values in the time-frequency plane). Note that the time-varying directed graph is an animating graph.

C. Discussion and Interpretation of the Results

The outcome of the time-varying dDTF measure using the simulated model shows that the mirror effect of the partial coherence on the ffDTF values causes erroneous results. This drawback of the dDTF measure can be explained by the effect of symmetric partial coherence matrix on the nonsymmetrical DTF matrix. In fact, the symmetry of the partial coherence matrix causes some reflections of the ffDTF elements about the diagonal. Also, very small values of the dDTF measures resulted from summation over frequencies in the denominator and multiplication of two smaller than one values makes the measure very small. Therefore, any comparison of the significant values between two channels becomes difficult. In contrast, the time-varying PDC is normalized between 0 and 1 and doesn't show any erroneous information.

According to Fig. 4, a unidirectional time-varying flow can be observed towards the left occipital and temporal lobes. The dominant flow starts roughly from C_z and P_3, two electrodes with maximum outflow and terminates at O_1, T_3 and T_5, three electrodes with maximum inflow. The result is in accordance with the outcome of a matching pursuit-based algorithm [14] which identifies P_3 as the seizure source (the results of the source localization will be published elsewhere). The strongest interaction occurs from O_1 to T_5 which suggests the effect of the seizure source on the primary visual cortex. Moreover, T_5 can be considered as the end point of the seizure for the considered time period, as there is no outflow from T_5 to the other channels.

The results also show that the time-varying version of the PDC based on DEKF exhibits high time-frequency resolution. In particular, DEKF seems capable of tracking the fast changing MVAR parameters for time-varying EEG signals. This is of high importance for seizure characterization, as rapid dynamic changes are observed in the epileptic EEG [15].

IV. CONCLUSION

The results presented in this paper show the superiority of the DEKF-based PDC in terms of its ability to track fast parameter changes and at the same time, accurately identify interactions compared to the dDTF using the simulated data. This advantage is valuable for characterizing EEG abnormalities such as seizure in the newborn, during which the dynamics change rapidly [15].

The findings also suggest that the time-varying cortical connectivity analysis may potentially lead to a source localization approach within the inner layers of the newborn brain. This would be a significant development in the neonatal EEG signal processing field of research, as adult EEG source localization methods are not applicable for analysis of neonatal brain interactions [16].

REFERENCES

[1] B. J. Fisch, *Fisch & Spehlmann's EEG primer: Basic principles of digital and analog EEG*, Amsterdam: Elsevier, 2005.

[2] G. L. Holmes, and C. T. Lombroso, "Prognostic Value of Background Patterns in the Neonatal EEG," *Journal of Clinical Neurophysiology,* vol. 10, no. 3, pp. 323-352, 1993.

[3] A. Aarabi, K. Kazemi, R. Grebe *et al.*, "Detection of EEG transients in neonates and older children using a system based on dynamic time-warping template matching and spatial dipole clustering," *Neuroimage,* vol. 48, no. 1, pp. 50-62, Oct, 2009.

[4] L. A. Baccalá, and K. Sameshima, "Partial directed coherence: a new concept in neural structure determination," *Biological Cybernetics,* vol. 84, no. 6, pp. 463-474, 2001.

[5] M. Kaminski, and K. Blinowska, "A new method of the description of the information flow in the brain structures," *Biological Cybernetics,* vol. 65, no. 3, pp. 203-210, 1991.

[6] A. Korzeniewska, M. Manczak, M. Kaminski *et al.*, "Determination of information flow direction among brain structures by a modified directed transfer function (dDTF) method," *Journal of Neuroscience Methods,* vol. 125, no. 1-2, pp. 195-207, 2003.

[7] R. Magjarevic, J. H. Nagel, Y. Ku *et al.*, "Nonstationary EEG Analysis using random-walk model," *World Congress on Medical Physics and Biomedical Engineering 2006*, IFMBE Proceedings R. Magjarevic, ed., pp. 1067-1070: Springer Berlin Heidelberg, 2007.

[8] B. Boashash, H. Carson, and M. Mesbah, "Detection of seizures in newborns using time-frequency analysis of EEG signals," in Statistical Signal and Array Processing, 2000. Proceedings of the Tenth IEEE Workshop on, 2000, pp. 564-568.

[9] E. A. Wan, and A. T. Nelson, "Neural dual extended Kalman filtering: applications in speech enhancement and monaural blind signal separation," in Neural Networks for Signal Processing [1997] VII. Proceedings of the 1997 IEEE Workshop, 1997, pp. 466-475.

[10] L. Sommerlade, K. Henschel, J. Wohlmuth *et al.*, "Time-variant estimation of directed influences during Parkinsonian tremor," *Journal of Physiology-Paris,* vol. 103, no. 6, pp. 348-352, 2009.

[11] A. Neumaier, and T. Schneider, "Estimation of parameters and eigenmodes of multivariate autoregressive models," *ACM Trans. Math. Softw.,* vol. 27, no. 1, pp. 27-57, 2001.

[12] W. Hesse, E. Möller, M. Arnold *et al.*, "The use of time-variant EEG Granger causality for inspecting directed interdependencies of neural assemblies," *Journal of Neuroscience Methods,* vol. 124, no. 1, pp. 27-44, 2003.

[13] E. Niedermeyer, and F. Lopes da Silva, *Electroencephalography: Basic Principles, Clinical Applications, and Related Fields* 5th ed.: Lippincott Williams & Wilkins, 2004.

[14] S. G. Mallat, and Z. Zhifeng, "Matching pursuits with time-frequency dictionaries," *Signal Processing, IEEE Transactions on,* vol. 41, no. 12, pp. 3397-3415, 1993.

[15] I. Gath, C. Feuerstein, D. T. Pham *et al.*, "On the tracking of rapid dynamic changes in seizure EEG," *Biomedical Engineering, IEEE Transactions on,* vol. 39, no. 9, pp. 952-958, 1992.

[16] N. Roche-Labarbe, A. Aarabi, G. Kongolo *et al.*, "High-resolution Electroencephalography and source localization in neonates," *Human Brain Mapping,* vol. 29, no. 2, pp. 167-176, Feb, 2008.